Asian Journal of Chemistry; Vol. 24, No. 5 (2012), 2073-2076

ASIAN JOURNAL OF CHEMISTRY

www.asianjournalofchemistry.co.in

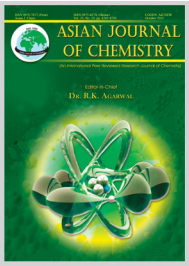

Simple Fabrication of Anatase-Brookite Mixed-Phase TiO_2 Nanoparticles with Visible-Light Responsive Photocatalytic Activity

BIN XUE*, TAO SUN and JI-KUI WU

Department of Chemistry, College of Food Science and Technology, Shanghai Ocean University, Shanghai 201306, P.R. China

*Corresponding author: Fax: +86 21 61900365; Tel: +86 21 61900363; E-mail: bxue@shou.edu.cn; binxue_chem@yahoo.com

(*Received*: 27 April 2011; *Accepted*: 12 December 2011) AJC-10831

Titanium dioxide (TiO_2) nanoparticles with binary mixed-phase were fabricated by a hydrothermal process under broad temperature range (100-180 ºC). The as-fabricated TiO_2 nanoparticles consist of rice-like nanocrystals with anatase-brookite mixed-phase. The ratios of anatase and brookite in the as-fabricated TiO_2 nanoparticles are affected by hydrothermal temperature. The absorption bands of the as-fabricated TiO_2 nanoparticles are distinctly red-shifted to visible light region. The as-fabricated TiO_2 nanoparticles exhibited the superior photocatalytic activity under visible light irradiation. Due to adoption of stable $TiCl_3$ as Ti sources, the fabrication route is simple and thus promotes large-scale production and application of mixed-phase TiO_2 nanoparticles for visible light driven photocatalytic process.

Key Words: Crystal structure, Nanomaterials, Semiconductors.

INTRODUCTION

Titanium dioxide (TiO_2), an environmentally friendly semiconductor material, is widely used in photocatalytic degradation of organic pollutants due to its high activity, low-cost, stability and non-toxic[1-4]. The crystal structure, morphology and size of TiO_2 significantly affect its photocatalytic activity. Titanium dioxide has three different crystalline polymorphs: anatase, rutile and brookite. Anatase phase of TiO_2 is generally considered more reactive than rutile and brookite in photocatalytic applications[1]. However, photocatalytic activity of anatase is too low under practical visible irradiation because of its wide band gap (3.2 eV)[1]. This problem seriously hinders extensive applications of TiO_2 in visible light driven photocatalytic process. Therefore, the design and fabrication of visible light responsive TiO_2 have attracted intense research interest.

Elements (metal or non-metal) doping, coupling with other semiconductor and crystalline phase mixing are conventional approaches to extend the photoresponse of TiO_2 to visible light range[5-11]. The above modified TiO_2 can effectively enhance the photocatalytic activity due to reduction of the recombination of photogenerated electros and holes. Among these various modified approaches, crystalline phase mixing has received increasing attention owing to facile process and highly active product[7-11]. For instance, Yu *et al.*[8] reported the sonochemical preparation of mesoporous TiO_2 with anatase and brookite using titanium isopropoxide as Ti sources and triblock copolymer as soft template. Zhang *et al.*[9] prepared TiO_2 nanocrystals with brookite and rutile mixed-phase using $TiCl_4$ as Ti sources under hydrothermal conditions. Paola *et al.*[10] synthesized binary or ternary crystalline phase mixtures of TiO_2 by thermohydrolysis of $TiCl_4$ in water. However, to the best of our knowledge, little work has been made to the fabrication of mixed-phase TiO_2 materials with visible-light responsive photocatalytic activity[11]. Therefore, it is still a challenge to fabrication of visible-light responsive TiO_2 materials with mixed-phase *via* a facile process on a large-scale.

In this study, we report the fabrication of anatase-brookite mixed-phase TiO_2 nanoparticles through a simple hydrothermal rote using stable $TiCl_3$ as Ti sources and hydrogen peroxide as assistant agent. The crystal phase, morphology, UV-VIS diffusive reflectance spectrum and visible-light responsive photocatalytic activity of mixed-phase TiO_2 nanoparticles were investigated.

EXPERIMENTAL

In a typical fabrication process, 8 mmol of $TiCl_3$ solution (16-18 %) was dissolved in 80 mL of deionized water, followed by adding 20 mmol of H_2O_2 solution (30 %). The mixture was stirred for 10 min then transferred into a 100 mL Teflon lined stainless steel autoclave, kept at a certain temperature for 12 h and then cooled naturally. The product was collected by centrifugation, washed using deionized water and dried 12 h at 80 ºC. The samples obtained at 100, 140 and 180 ºC are denoted as S-100, S-140 and S-180, respectively.

TABLE-1
PARAMETERS OF THE AS-FABRICATED SAMPLES AND P25

Samples	Anatase		Brookite		Particle size[b] (nm)		Optical band gap energy (eV)
	Content (%)	Crystalline size[a] (nm)	Content (%)	Crystalline size[a] (nm)	Width	Length	
S-100	66.1	9.6	33.9	12.2	5.0	12	2.98
S-140	65.4	10.0	34.6	14.9	7.5	15	2.99
S-180	56.8	10.2	43.2	17.2	15	20	3.04
P25	-	-	-	-	-	-	3.10

a. Calculated by XRD pattern using the Scherrer equation; b. Measured from TEM images

The X-ray powder diffraction (XRD) pattern of the samples was recorded using a PAN analytical X'Pert PRO diffractometer. Transmission electron microscopy (TEM) was performed on PHILIPS CM200 microscope. UV-VIS diffusive reflectance spectrum of the product was obtained on a UV-Visible spectrophotometer (Shimadzu UV-2550) and $BaSO_4$ was used as a reference.

In a typical photocatalytic activity measurement, 50 mg of samples was added to 50 mL of a 10 mg L^{-1} methyl orange (MO) solution (adjust the pH to 3.4 with 2 mol L^{-1} HCl) and then stirred in the dark for 0.5 h to ensure an adsorption equilibrium. The suspension was then exposed to visible-light irradiation from a 250 W mercury blended lamp with a filter (> 420 nm). After various reaction times, samples were removed by centrifugation and the solution concentrations were analyzed using a UV-VIS spectrophotometer (UV-2550, Shimadzu).

RESULTS AND DISCUSSION

Fig. 1 shows the XRD pattern of the as-fabricated samples. The patterns are well-indexed to the mixture phase of anatase (JCPDS No. 21-1272) and brookite (JCPDS No. 29-1360) of TiO_2. No diffraction peaks of other phases or impurities appeared in the patterns. The phase content in the samples can be calculated using the following equations:[8]

$$W_A = \frac{k_A A_A}{k_A A_A + k_B A_B} \quad (1)$$

$$W_B = \frac{k_B A_B}{k_A A_A + k_B A_B} \quad (2)$$

where, W_A and W_B represent the weight fractions of anatase and brookite, respectively. A_A and A_B represent the integrated intensities of the anatase (101) and brookite (121) diffraction peaks, respectively. Coefficient k_A and k_B are 0.886 and 2.721, respectively. On the basis of the width of the anatase (101) and brookite (121) diffraction peaks, the average crystallite sizes of the anatase and brookite phase were calculated using the Scherrer equation. The calculated phase contents and the average crystallite size of the as-fabricated samples are summarized in Table-1. With increasing hydrothermal temperature, the brookite phase components of the as-fabricated samples gradually increase and the average crystallite sizes of the brookite phase obviously increase. The anatase phase components of the as-fabricated samples gradually decrease along the increase of temperature and corresponding increasing trend of the anatase phase sizes is unapparent. It is obvious that the ratios of anatase and brookite in the as-fabricated samples can be readily tuned with hydrothermal temperature.

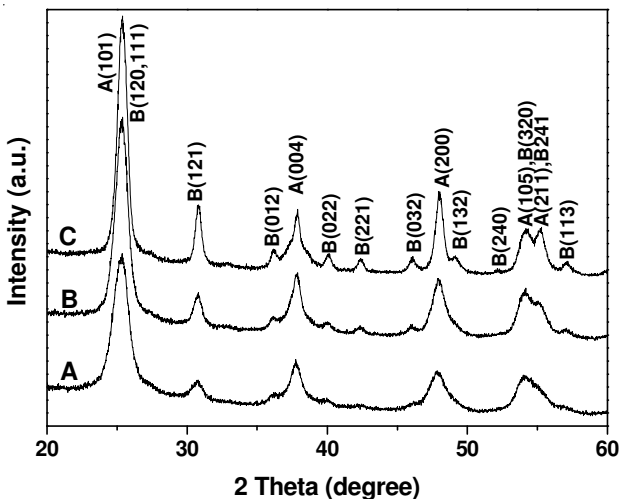

Fig. 1. XRD pattern of S-100 (A), S-140 (B) and S-180 (C)

Fig. 2 is the representative TEM and HRTEM images of the as-fabricated samples. The particle sizes of the as-fabricated samples measured from TEM images are listed in Table- 1. As shown in Figs. 2a, b and c, the as-fabricated samples all consist of rice-like nanoparticles. The size of nanoparticles is close to the crystal size calculated by the Scherrer equation from XRD pattern in Fig. 1 with increasing hydrothermal temperature, aspect ratios of the as-fabricated samples gradually increase. Fig. 2d shows clear crystalline lattice fringes in the HRTEM image of S-140. The lattice spacings of 0.325 and 0.290 nm correspond to the (101) crystal plane of the anatase lattice and the (121) crystal plane of the brookite lattice, respectively. The HRTEM images of S-100 and S-180 also display analogous feature (data not shown), indicating the as-fabricated samples under various temperatures are well-crystallized.

The UV-VIS diffusive reflectance spectrum of the as-fabricated samples and P25 TiO_2 nanoparticles are shown in Fig. 3. The absorption bands of the as-fabricated samples under various temperatures are distinctly red-shifted compared to that of P25 and absorption band edges of the as-fabricated samples gradually extended to 800 nm. The corresponding optical band gap energy data are summarized in Table-1. With increasing the brookite phase components, optical band gap energy of the as-fabricated samples gradually increase. How ever, optical band gap energies of whole as-fabricated samples are less than that of P25. The narrowing appearance of optical band gap has been widely reported in the literatures about TiO_2 nanoparticles with mixed crystalline structure[7-11]. Therefore, the unique phenomenon of the optical absorption in the as-fabricated samples may be related to their anatase-brookite mixed crystalline structure and narrowing optical band gap.

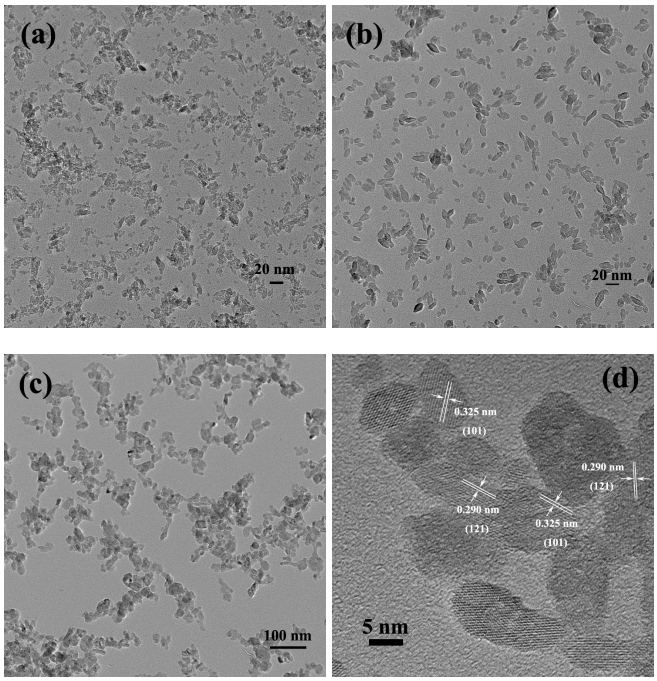

Fig. 2. Representative TEM images of S-100 (a), S-140 (b), S-180 (c) and HRTEM image of S-140 (d)

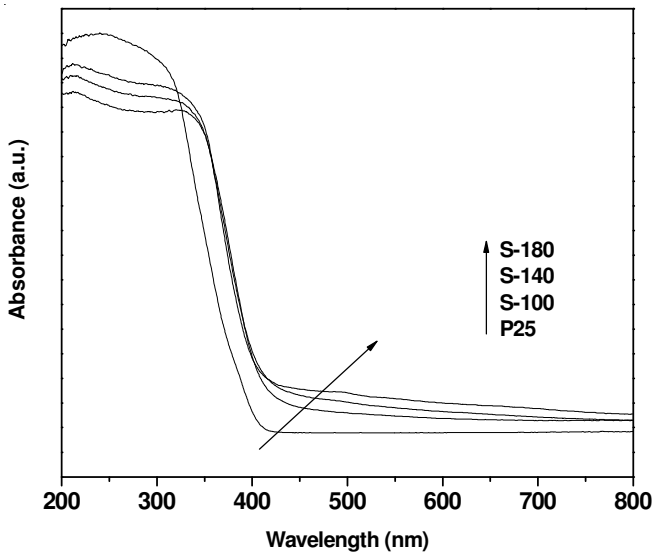

Fig. 3. UV-VIS diffusive reflectance spectrum of the as-fabricated samples and P25 TiO_2 nanoparticles

The photocatalytic activity of the as-fabricated samples was evaluated by degradation of methyl orange solution under visible light irradiation. The characteristic absorption of methyl orange solution at 499 nm on the UV-VIS absorption spectra was selected to determine its concentration. Fig. 4 shows time curves of photocatalytic degradation of methyl orange solution for five different samples. Without any catalyst, the concentrations of methyl orange solution are almost unchanged under visible light irradiation. However, the as-fabricated samples obviously exhibited superior photocatalytic activity under the same experimental conditions. P25 shows the lower photocatalytic activity than the as-fabricated samples. The photocatalytic degradation efficiency of methyl orange on different TiO_2 nanoparticles under visible light irradiation follows the order: S-100 ≈ S-140 > S-180 >> P25. As is well know, the coupling of different TiO_2 polymorphs possessing different redox energies can effectively reduce the recombination of photogenerated electrons and holes to enhance the photocatalytic activity. Once excited, photogenerated electrons transferred from the conduction band of anatase to that of brookite, while photogenerated holes transferred from the valence band of brookite to that of anatase, which hinders the photogenerated electro-hole recombination. In addition, it has been reported that small grains of brookite TiO_2 (size less than 25 nm) exhibited high photocatalytic activity.[8,12] Consequently, the superior photocatalytic activity of the as-fabricated samples could be attributed to mixed crystalline structure of anatase and brookite.

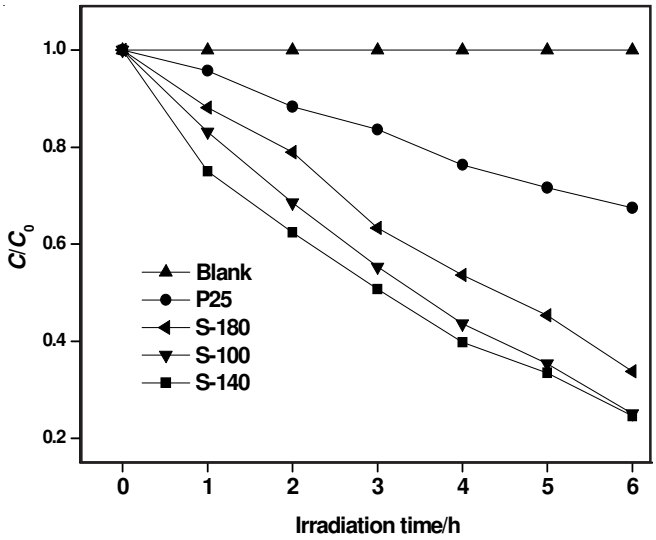

Fig. 4. Photocatalytic activity of the as-fabricated samples and P25

Conclusion

We have successfully fabricated TiO_2 nanoparticles with anatase-brookite mixed-phase *via* a simple hydrothermal route using stable $TiCl_3$ as Ti sources. The as-fabricated TiO_2 nanoparticles exhibited the distinct red-shift phenomenon in UV-VIS diffusive reflectance spectrum. The as-fabricated TiO_2 nanoparticles show better visible light photocatalytic activity than P25 TiO_2. The binary mixed-phase TiO_2 nanoparticles are expected for practical applications in visible light induced photocatalytic degradation of organic pollutants and disinfection of drinking water.

ACKNOWLEDGEMENTS

This work was financially supported by Special Science and Technology Research Funds for Shanghai Universities and Colleges to Select and Foster Excellent Young Teachers (Grant No. ssc09021), Leading Academic Discipline Project of Shanghai Municipal Education Commission (Project Number: J50704), Initial Doctoral Funding of Shanghai Ocean University (Grant No.A-2400-10-0131), the Natural Science Foundation of Shanghai, China (no.11ZR1415400) and Zhaoyao Luo Students Technology Innovation Funds of Shanghai Ocean University (Project: A-2900-10-001110).

REFERENCES

1. X.B. Chen and S.S. Mao, *Chem. Rev*., **107**, 2891 (2007).
2. J. Hu, C. Zhang, S. Guan, L. Wang, S. Zhu, S. Chen, J. Gao, E. Meng, S. Hou, B. Cui and H. Sun, *Mater. Lett*., **64**, 2569 (2010).
3. C.Y. Hu, S.W. Duo, R.F. Zhang, M.S. Li, J.H. Xiang and W.K. Li, *Mater. Lett*., **64**, 2040 (2010).
4. M.X. Xia, Y.C. Wang, H.X. Li, Y.P. Zeng, B.H. Qu, F.X. Wang, A.L. Pan, B.S. Zou, Q.L. Zhang and Y.G. Wang, *Mater. Lett*., **64**, 2392 (2010).
5. M. Hamadanian, A. Reisi-Vanani and A. Majedi, *Mater. Chem. Phys*., **116**, 376 (2009).
6. J.G. Li, T. Ishigaki and X.D. Sun, *J. Phys. Chem. C*, **111**, 4969 (2007).
7. J.Y. Li, S.L. Xiong, J. Pan and Y.T. Qian, *J. Phys. Chem. C*, **114**, 9645 (2010).
8. J.C. Yu, L.Z. Zhang and J.G. Yu, *Chem. Mater*., **14**, 4647 (2002).
9. H. Xu and L.Z. Zhang, *J. Phys. Chem. C*, **113**, 1785 (2009).
10. A.D. Paola, M. Bellardita, R. Ceccato, L. Palmisano and F. Parrino, *J. Phys. Chem. C*, **113**, 15166 (2009).
11. L. Li and C.Y. Liu, *Eur. J. Inorg. Chem*., 3727 (2009).
12. B. Ohtani, J.I. Handa, S.I. Nishimoto and T. Kagiya, *Chem. Phys. Lett*., **120**, 292 (1985).